genes besides *TEP1* must contribute. This is apparent from comparing phenotypes of groups from different generations with the same *TEP1* genotypes (Figs. 1B and 4A): For instance, 50 to 70% of **R1/R2* and **R1/S2* mosquitoes were resistant in F2, whereas <7% were resistant in F1. Thus, this additional locus (or loci) appears to be unlinked to TEP1 and also to have a limited impact in mosquitoes homozygous for the extreme alleles **R1* and **S2*, which have similar resistance as the parental strains but are essential to support resistance in heterozygotes. Future work may focus on identifying secondary QTL(s) and potential candidate *TEP1* suppressor gene(s).

The single locus identified here that controls resistance to *P. berghei* and includes *TEP1* does not overlap with previously reported QTLs controlling the intensity of infection of natural populations by the human malaria parasite *P. falciparum*, and in particular, does not overlap with the major *Plasmodium* resistance island (PRI) (*16–18*) (Fig. 1C). Two leucine-rich repeat proteins encoded in the PRI, APL1 and LRIM1, form a complex with TEP1. These proteins maintain mature TEP1 in circulation and regulate its binding to parasites and their subsequent killing (*19, 20*). Polymorphisms in TEP1 itself or in proteins that control TEP1 function might both contribute to the efficiency of TEP1 antiparasitic activity. The differences between the QTLs identified in laboratory strains and in field mosquitoes might thus reflect the sampling of determinant polymorphism(s) in various players of the same pathway, rather than different mechanisms employed to limit development of human and rodent malaria parasite species. Consistently, silencing of *TEP1* increases *A. gambiae* susceptibility to both murine and human *Plasmodia* (*5, 21*). Haplotypes of the susceptible and resistant alleles of *TEP1*, as well as recombinants between these forms, exist in field populations from East and West Africa (*22*). Understanding the genetic basis of resistance to malaria parasites, as well as how the determinant polymorphisms are maintained and selected in field populations, will be of tremendous importance for the control of malaria transmission.

References and Notes

1. F. H. Collins *et al.*, *Science* **234**, 607 (1986).
2. K. D. Vernick *et al.*, *Exp. Parasitol.* **80**, 583 (1995).
3. L. Zheng *et al.*, *Science* **276**, 425 (1997).
4. L. Zheng *et al.*, *BMC Genet.* **4**, 16 (2003).
5. S. Blandin *et al.*, *Cell* **116**, 661 (2004).
6. J. Volz, H. M. Muller, A. Zdanowicz, F. C. Kafatos, M. A. Osta, *Cell. Microbiol.* **8**, 1392 (2006).
7. S.-H. Shiao, M. M. A. Whitten, D. Zachary, J. A. Hoffmann, E. A. Levashina, *PLoS Pathog.* **2**, e133 (2006).
8. B. Franke-Fayard *et al.*, *Mol. Biochem. Parasitol.* **137**, 23 (2004).
9. Materials and methods are available as supporting material on *Science* Online.
10. M. J. Gorman, S. M. Paskewitz, *Am. J. Trop. Med. Hyg.* **56**, 446 (1997).
11. R. M. Waterhouse *et al.*, *Science* **316**, 1738 (2007).
12. S. A. Blandin, E. Marois, E. A. Levashina, *Cell Host Microbe* **3**, 364 (2008).
13. R. H. Baxter *et al.*, *Proc. Natl. Acad. Sci. U.S.A.* **104**, 11615 (2007).
14. E. A. Levashina *et al.*, *Cell* **104**, 709 (2001).
15. L. M. Steinmetz *et al.*, *Nature* **416**, 326 (2002).
16. O. Niaré *et al.*, *Science* **298**, 213 (2002).
17. M. M. Riehle *et al.*, *Science* **312**, 577 (2006).
18. M. M. Riehle *et al.*, *PLoS One* **3**, e3672 (2008).
19. M. Fraiture *et al.*, *Cell Host Microbe* **5**, 273 (2009).
20. M. Povelones, R. M. Waterhouse, F. C. Kafatos, G. K. Christophides, *Science* **324**, 258 (2009); published online 4 March 2009 (10.1126/science.1171400).
21. Y. Dong *et al.*, *PLoS Pathog.* **2**, e52 (2006).
22. D. J. Obbard *et al.*, *BMC Evol. Biol.* **8**, 274 (2008).
23. We thank A. Cohuet for sharing sequencing information, R. Carmouche and J. Luis from the EMBL Genecore facility for support with genotyping, R. Bourgon for advice on statistical analyses, A. Budd for suggestions on the phylogenetic analysis, D. Doherty and J. Soichot for help with breeding mosquitoes, and E. Marois and C. Ramakrishnan for comments on the manuscript. We acknowledge the support of F. Kafatos, in whose laboratory this work was initially carried out. This work was supported by grants from NIH and the Deutsche Forschungsgemeinschaft (L.M.S.), CNRS and INSERM (E.A.L. and S.A.B), the European Molecular Biology Organization (EMBO) Young Investigators Program (E.A.L.), and the European Commission Network of Excellence "BioMalPar" (E.A.L.). S.A.B. received a postdoctoral fellowship from EMBO. E.A.L. is an international Howard Hughes Medical Institute research scholar. EMBL Nucleotide Sequence Database accession numbers for *TEP1* alleles sequenced in this report are as follows: FN431782 to FN431785.

Coat Variation in the Domestic Dog Is Governed by Variants in Three Genes

Edouard Cadieu,[1] Mark W. Neff,[2] Pascale Quignon,[1] Kari Walsh,[2] Kevin Chase,[3] Heidi G. Parker,[1] Bridgett M. VonHoldt,[4] Alison Rhue,[2] Adam Boyko,[5] Alexandra Byers,[1] Aaron Wong,[2] Dana S. Mosher,[1] Abdel G. Elkahloun,[1] Tyrone C. Spady,[1] Catherine André,[6] K. Gordon Lark,[3] Michelle Cargill,[7]* Carlos D. Bustamante,[5] Robert K. Wayne,[4] Elaine A. Ostrander[1]†

Coat color and type are essential characteristics of domestic dog breeds. Although the genetic basis of coat color has been well characterized, relatively little is known about the genes influencing coat growth pattern, length, and curl. We performed genome-wide association studies of more than 1000 dogs from 80 domestic breeds to identify genes associated with canine fur phenotypes. Taking advantage of both inter- and intrabreed variability, we identified distinct mutations in three genes, *RSPO2*, *FGF5*, and *KRT71* (encoding R-spondin–2, fibroblast growth factor–5, and keratin-71, respectively), that together account for most coat phenotypes in purebred dogs in the United States. Thus, an array of varied and seemingly complex phenotypes can be reduced to the combinatorial effects of only a few genes.

The tremendous phenotypic diversity of modern dog breeds represents the end point of a >15,000-year experiment in artificial and natural selection (*1, 2*). As has been demonstrated for traits such as body size (*3*) and coat color (*4*), marker-based associations with phenotypic traits can be explored within single breeds to initially identify regions of genetic association, and then expanded to multiple breeds for fine-mapping and mutation scanning (*5, 6*).

Coat (pelage) phenotypes are particularly amenable to this strategy as they show a huge amount of variation across breeds but still allow for simple variation within single breeds (*7*). This offers a unique strategy for advancing the genetic understanding of a complex phenotype.

We used the structured pattern of fur variation in dogs to localize the genetic basis of three characteristics of the canine coat: (i) the presence or absence of "furnishings," the growth pattern marked by a moustache and eyebrows typically observed in wire-haired dogs; (ii) hair length; and (iii) the presence or absence of curl. To accomplish this, we generated three genome-wide single-

[1]National Human Genome Research Institute, National Institutes of Health, Bethesda, MD 20892, USA. [2]Veterinary Genetics Laboratory, University of California, Davis, CA, 95616, USA. [3]Department of Biology, University of Utah, Salt Lake City, UT 84112, USA. [4]Department of Ecology and Evolutionary Biology, University of California, Los Angeles, CA, 90095, USA. [5]Department of Biological Statistics and Computational Biology, Cornell University, Ithaca, NY 14853, USA. [6]UMR 6061, CNRS, Université de Rennes 1, Faculté de Médecine, CS 34317, Rennes, France. [7]Affymetrix Corporation, Santa Clara, CA 95051, USA.

*Present address: Genetics Navigenics, Foster City, CA 94404, USA.
†To whom correspondence should be addressed. E-mail: eostrand@mail.nih.gov

nucleotide polymorphism (SNP) data sets using the Affymetrix version 2.0 canine SNP chip (8, 9). The first data set consisted of 96 dachshunds segregating three coat varieties: wire-haired with furnishings, smooth, and long-haired without furnishings. The second data set comprised 76 Portuguese water dogs (PWDs), segregating the curl phenotype. The final data set, termed CanMap, included 903 dogs from 80 breeds representing a wide variety of phenotypes. An additional data set used to map furnishings included a panel of microsatellite markers (10), genotyped on a 96-dachshund pedigree segregating all three coat varieties.

The same strategy was used to map all three traits. First, a genome-wide association study (GWAS) within a breed segregating the phenotype was conducted to determine the most strongly associated locus. To rule out false-positives caused by population structure within the breeds (11), we did a second GWAS that used the CanMap data set divided into cases and controls based on the presence or absence of the phenotype in question. Fine-mapping of significant, concordant peaks was used to define the smallest shared haplotype, followed by sequencing to identify the putative causative mutations. Each mutation was validated in a large panel of at least 661 dogs from 108 breeds, including cases and controls for all phenotypes (table S1).

We initially mapped furnishings in the dachshund using smooth-coated and long-haired dogs as controls and wire-haired dogs as cases (Fig. 1A). Single-marker analysis of the dachshund GWAS data set and concurrent linkage analysis of the dachshund pedigree identified the same locus on canine chromosome 13 (CFA13) surrounding nucleotide 11,095,120 [$P = 3.4 \times 10^{-27}$, lod score (logarithm of the odds ratio for linkage) = 5.6; Fig. 1B]. We confirmed the association on CFA13 in the CanMap data set at nucleotide 11,659,792 ($P = 10^{-241}$; Fig. 1C and table S2). A 718-kb homozygous haplotype in all dogs fixed with furnishings was located within both the original 3.4-Mb haplotype observed in the dachshund-only GWAS, and a 2.8-Mb haplotype identified in crossover analysis within the dachshund pedigree (Fig. 1D).

Fine-mapping allowed us to reduce the homozygous region to 238 kb spanning only the R-spondin–2 (RSPO2) gene, excluding the 5′ untranslated region (5′UTR) and the first exon (Fig. 1D, fig. S1, and table S3). RSPO2 is an excellent candidate for a hair-growth phenotype as it synergizes with Wnt to activate β-catenin (12), and Wnt signaling is required for the establishment of the hair follicles (13, 14). Moreover, the Wnt/β-catenin pathway is involved in the development of hair-follicle tumors, or pilomatricomas (15), which occur most frequently in breeds that have furnishings (16). Recent studies have shown that a mutation in the EDAR gene, also involved in the Wnt pathway, is responsible for a coarse East-Asian hair type found in humans (17), with some similarity to canine wirehair.

All exons and conserved regions of RSPO2 were sequenced in dogs from seven breeds (table S4). Only an insertion of 167 base pairs (bp) within the 3′UTR at position 11,634,766 was perfectly associated with the furnishings trait in dogs from both the case/control study and the extended pedigree (table S5). The result was further confirmed in a set of 704 dogs of varying phenotypes. In total, 297 of 298 dogs with furnishings were either homozygous (268) or heterozygous (29) for the insertion, and all 406 dogs lacking the trait were homozygous for the ancestral state, as is consistent with a dominant mode of inheritance (table S1).

This mutation does not affect the protein-coding region of the RSPO2 gene. However, because the 3′UTR frequently encodes elements that influence mRNA stability [reviewed in (18)], we examined whether the insertion was associated with a change in the expression level of the RSPO2 gene. We found a threefold increase in RSPO2 transcripts in muzzle skin biopsies of dogs with furnishings, consistent with a transcript effect (fig. S2).

We applied the same mapping strategy to hair length. Previously, mutations in the FGF5 gene were identified in Welsh corgis segregating an atypical "fluffy" or long-haired phenotype (19) and associated with excess hair growth in mice and cats (20–22). Our study replicates these findings in an extended breed set. Indeed, association analyses in both the dachshund and CanMap data sets highlight the region on CFA32 containing FGF5 with P values of 3×10^{-27} and 9×10^{-44}, respectively. After fine-mapping, a 67-kb homozygous region highlighted the FGF5 gene (Fig. 2A, fig. S3, and table S6). The strongest association was observed at position 7,473,337 ($P = 1 \times 10^{-157}$), in which a highly conserved Cys is changed to Phe (Cys^{95}→Phe) in exon 1 of FGF5, consistent with the previous study (19). Sequencing within the homozygous haplotype revealed no SNPs with stronger association (table S7).
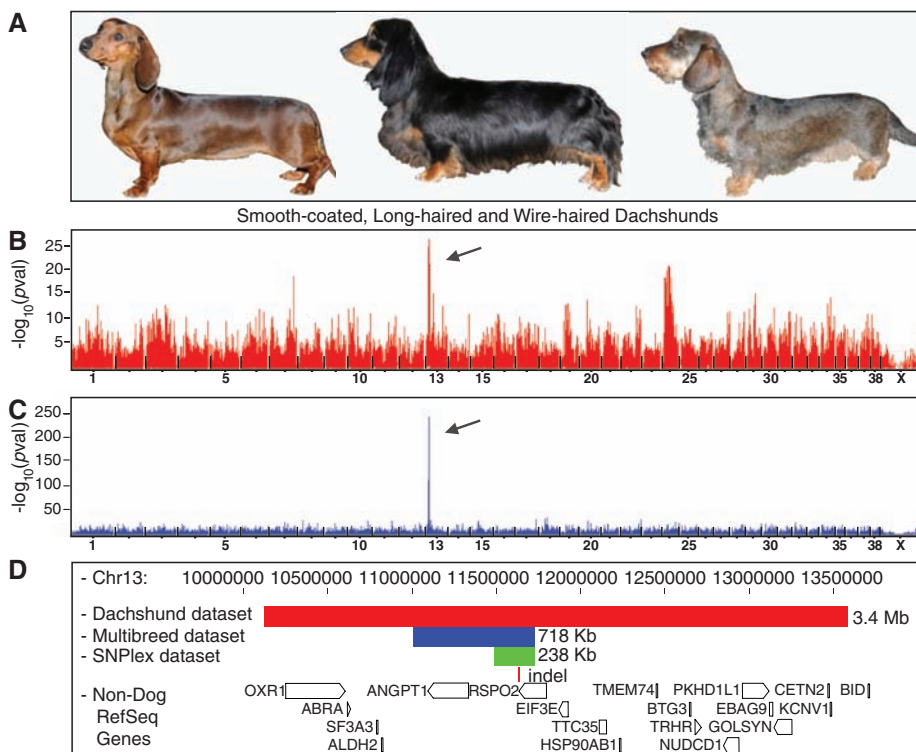

Fig. 1. GWAS and fine-mapping identify *RSPO2* as the associated gene for moustache and eyebrow growth pattern (furnishings). (**A**) Three types of coat segregate in dachshunds: (from left to right) smooth-coated, long-haired, and wire-haired with furnishings. (**B**) Results of the GWAS in the dachshund using wire-haired dogs as cases and smooth-coated and long-haired dogs as controls. The best *P* value (3.35 × 10^{-27}), highlighted by the arrow, is located on CFA13 at position 11,095,120. (**C**) Results of the GWAS for furnishings in the CanMap data set. The arrow highlights the best association (*P* = 10^{-241}) at CFA13 position 11,659,792. Both *P* values were obtained with single-marker χ^2 analyses. (**D**) Homozygous regions identified in cases from GWAS and fine-mapping. The red rectangle represents the associated haplotype in the dachshund; the blue rectangle spans the homozygous region from 19 breeds fixed for furnishings based on the multibreed data set; the green rectangle indicates the region of homozygosity in 18 breeds fixed for the furnishings after fine-mapping. A 167-bp deletion, indicated by the small red rectangle, is located within all three haplotypes in the 3′UTR of the *RSPO2* gene. The positions of genes in the region are represented by open boxes at the bottom of the figure, labeled to the left, with arrows indicating reading-frame direction (www.genome.ucsc.edu).
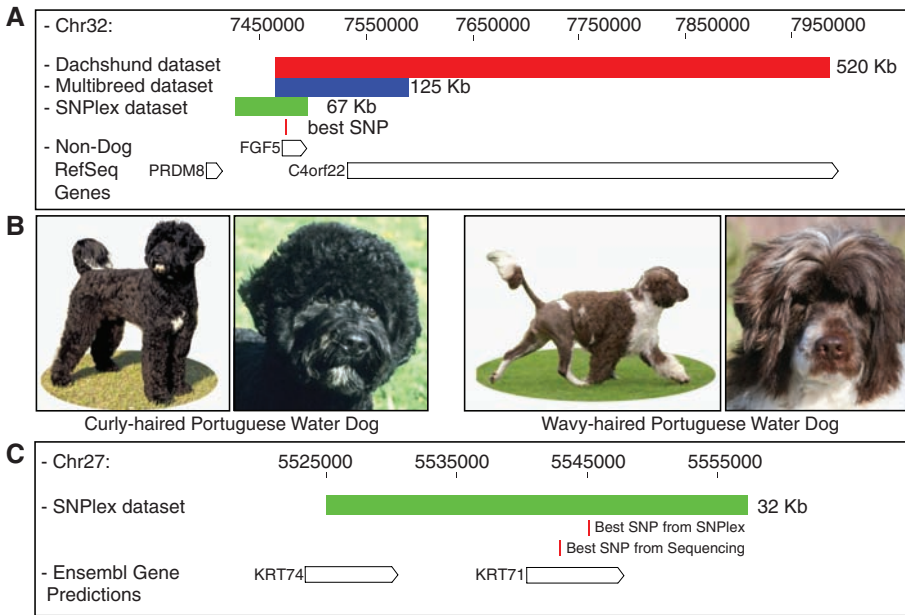
Fig. 2. Regions of homozygosity identify genes for pelage length and curl. (**A**) Homozygous region found on CFA32 defining the length locus. The red bar indicates the 520-kb associated haplotype from 29 long-haired dachshunds; the blue bar spans the 125-kb homozygous region found in 319 dogs from 31 long-haired breeds; the green bar represents the 67-kb reduced homozygous region found after fine-mapping in 293 dogs from 39 long-haired breeds. The best-associated SNP, represented by the small red rectangle, is within these three homozygous regions in exon 1 of the *FGF5* gene. (**B**) PWDs display two coat varieties: curly (two left panels) and wavy (two right panels). (**C**) Haplotype analysis at the curl locus on CFA27. The green bar represents the 32-kb homozygous haplotype found after fine-mapping in 65 dogs from five curly haired breeds. The best-associated SNP, represented by the small red rectangle, was found within the homozygous haplotype in exon 2 of the *KRT71* gene. The positions of genes in both regions (A and C) are represented by open boxes at the bottom of each figure, labeled to the left, with arrows indicating reading-frame direction (www.genome.ucsc.edu). Curly PWD photos courtesy of M. Bloom (Copyright AKC).
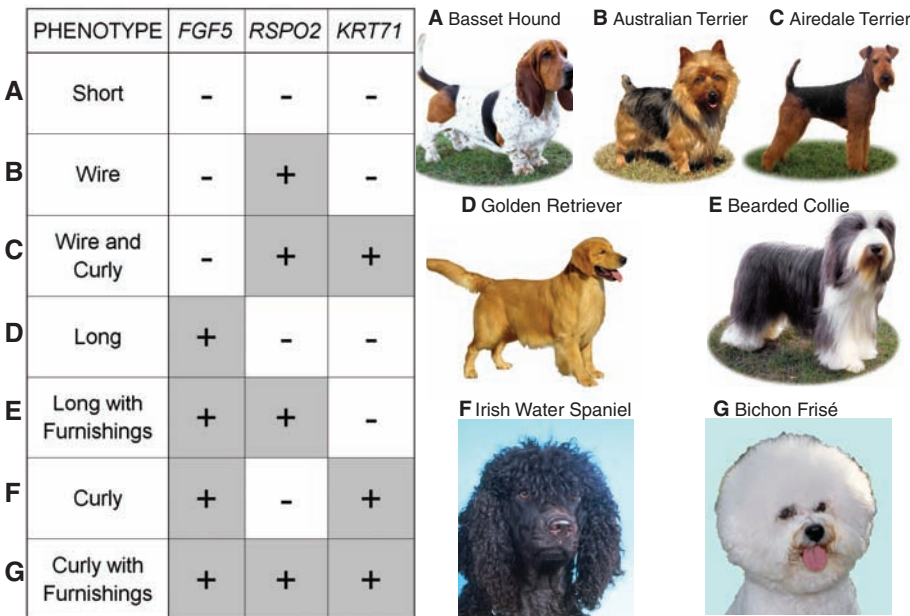

Fig. 3. Combinations of alleles at three genes create seven different coat phenotypes. Plus (+) and minus signs (–) indicate the presence or absence of variant (nonancestral) genotype. A characteristic breed is represented for each of the seven combinations observed in our data set: (**A**) short hair; (**B**) wire hair; (**C**) "curly-wire" hair; (**D**) long hair; (**E**) long, soft hair with furnishings; (**F**) long, curly hair; and (**G**) long, curly hair with furnishings. [Photos courtesy of M. Bloom (Copyright AKC)].

This diagnostic SNP was typed in several hundred additional dogs of varying hair length. Within the dachshunds, all long-haired dogs had the TT genotype, whereas all short or wire-haired dogs had either the GT or GG genotypes, suggesting a recessive mode of inheritance, as predicted previously (*23*). Across all breeds, the T allele was found in 91% of the long-haired dogs, in only 3.9% of the short-haired dogs, and accounts for ~30% of genotypes found in medium-haired dogs. Three breeds with very long hair, including the Afghan hound, neither carry the Cys[95]→Phe variant nor show an association with CFA32, suggesting that additional loci exist that contribute to hair length in dogs (table S1).

To identify the gene that causes curly coat, we conducted a GWAS using PWDs (Fig. 2B) and identified a single associated SNP at position 5,444,030 on CFA27 ($P = 4.5 \times 10^{-7}$). A SNP in close proximity (5,466,995; $P = 6.9 \times 10^{-28}$) was associated with curly coat in the CanMap data set. Fine-mapping revealed a shared homozygous haplotype that included two keratin genes (Fig. 2C, fig. S4, and table S8). Sequence data covering 87% of the homozygous region identified one SNP at position 5,542,806 that segregated with the trait. Non–curly haired dogs carried the CC genotype; curly coated dogs had the TT genotype. In breeds where the trait segregates, such as PWDs, all three genotypes were observed. The relevant SNP is located in the *KRT71* gene (previously called K6irs1, Kb34, and K71) and causes a nonsynonymous Arg[151]→Trp alteration (table S9). Genotyping an additional 661 samples at this SNP validated the association ($P = 3 \times 10^{-92}$) (table S1).

Keratins are obvious candidates for hair growth [reviewed in (*24*)], and mutations in *KRT71* have been described in curly coated mice (*25*). The mutation described in our study is within the second exon of the gene and may affect either or both of two protein domains: a coiled-coil and a prefoldin domain (www.ensembl.org/Canis_familiaris/). Conceivably, sequence alterations in these domains could affect cellular targeting, receptor binding, or proper folding of the protein after translation [reviewed in (*26*)].

Notably, these three mutations in various combinations explain the observed pelage phenotype of 95% of dogs sampled, which include 108 of the ~160 American Kennel Club (AKC)–recognized breeds. A total of 622 dogs representing all identifiable coat phenotypes were genotyped at all three loci (table S10). By analyzing each of the three major traits both within and across multiple breeds, we show that combinations of these genotypes give rise to at least seven different coat types, encompassing most coat variation in modern domestic dogs (Fig. 3). Specifically, short-haired breeds display the ancestral state in all three genes. Wire-haired breeds, all of which have furnishings, carry the *RSPO2* insertion. Dogs that carry both the *RSPO2* and *KRT71* mutations display "curly-wire" hair that is similar in texture to wire-hair but longer

and curled or kinked rather than straight. Long-haired breeds carry the variant form of *FGF5*. Dogs carrying the *FGF5* mutation, along with the *RSPO2* insertion, have furnishings and long soft coats, rather than wiry ones. When dogs carry variants in both *FGF5* and *KRT71*, the pelage is long and curly. Not surprisingly, coats must be of sufficient length to curl, and all curly haired dogs in our study were homozygous for the *FGF5* mutation. Finally, if all three mutations are present, the phenotype is long and curly with furnishings.

None of the mutations we observed were found in three gray wolves or the short-haired dogs, indicating that short-haired dogs carry the ancestral alleles (table S1). Our finding of identical haplotypes surrounding the variants in all dogs displaying the same coat type suggests that a single mutation occurred for each trait and was transferred multiple times to different breeds through hybridization. Because most breeds likely originated within the past 200 years (*27*), our results demonstrate how a remarkable diversity of phenotypes can quickly be generated from simple genetic underpinnings. Consequently, in domesticated species, the appearance of phenotypic complexity can be created through combinations of genes of major effect, providing a pathway for rapid evolution that is unparalleled

in natural systems. We propose that in the wake of artificial selection, other complex phenotypes in the domestic dog will have similar tractable architectures that will provide a window through which we can view the evolution of mammalian form and function.

References and Notes

1. C. Vila *et al.*, *Science* **276**, 1687 (1997).
2. P. Savolainen, Y. P. Zhang, J. Luo, J. Lundeberg, T. Leitner, *Science* **298**, 1610 (2002).
3. N. B. Sutter *et al.*, *Science* **316**, 112 (2007).
4. E. K. Karlsson *et al.*, *Nat. Genet.* **39**, 1321 (2007).
5. K. Lindblad-Toh *et al.*, *Nature* **438**, 803 (2005).
6. R. K. Wayne, E. A. Ostrander, *Trends Genet.* **23**, 557 (2007).
7. American Kennel Club, *The Complete Dog Book*. (Howell Book House, New York, NY, ed. 19th Edition Revised, 1998).
8. C. Drogemuller *et al.*, *Science* **321**, 1462 (2008).
9. Materials and methods can be found at *Science* Online.
10. A. K. Wong, M. W. Neff, *Anim. Genet.* **40**, 569 (2009).
11. E. S. Lander, N. J. Schork, *Science* **265**, 2037 (1994).
12. O. Kazanskaya *et al.*, *Dev. Cell* **7**, 525 (2004).
13. T. Andl, S. T. Reddy, T. Gaddapara, S. E. Millar, *Dev. Cell* **2**, 643 (2002).
14. H. Clevers, *Cell* **127**, 469 (2006).
15. E. F. Chan, U. Gat, J. M. McNiff, E. Fuchs, *Nat. Genet.* **21**, 410 (1999).
16. D. J. Meuten, Ed., *Tumors in Domestic Animals* (Blackwell, Ames, Iowa, ed. 4, 2002).
17. C. Mou *et al.*, *Hum. Mutat.* **29**, 1405 (2008).
18. S. Chatterjee, J. K. Pal, *Biol. Cell* **101**, 251 (2009).
19. D. J. Housley, P. J. Venta, *Anim. Genet.* **37**, 309 (2006).
20. J. P. Sundberg *et al.*, *Vet. Pathol.* **34**, 171 (1997).
21. C. Drogemuller, S. Rufenacht, B. Wichert, T. Leeb, *Anim. Genet.* **38**, 218 (2007).
22. J. M. Hebert, T. Rosenquist, J. Gotz, G. R. Martin, *Cell* **78**, 1017 (1994).
23. C. R. Stockard, *The Genetic and Endocrinic Basis for Differences in Form and Behavior* (The Wistar Institute of Anatomy and Biology, Philadelphia, 1941).
24. L. Langbein, J. Schweizer, *Int. Rev. Cytol.* **243**, 1 (2005).
25. F. Runkel *et al.*, *Mamm. Genome* **17**, 1172 (2006).
26. J. Martin, M. Gruber, A. N. Lupas, *Trends Biochem. Sci.* **29**, 455 (2004).
27. E. C. Ash, *Dogs: Their History and Development* (Benn, London, 1927).
28. We gratefully acknowledge support from NSF grants 0733033 (R.K.W.) and 516310 (C.D.B.), NIH grants 1RO1GM83606 (C.D.B.) and GM063056 (K.G.L. and K.C.), the Nestlé Purina company, the AKC Canine Health Foundation, the University of California–Davis Veterinary Genetics Laboratory, and the Intramural Program of the National Human Genome Research Institute. We thank L. Warren and S. Stafford for providing pictures. Finally, we thank the many dog owners who generously provided us with samples from their pets.

JAK-STAT Signal Inhibition Regulates Competition in the *Drosophila* Testis Stem Cell Niche

Melanie Issigonis, Natalia Tulina,* Margaret de Cuevas, Crista Brawley,†
Laurel Sandler, Erika Matunis‡

Adult stem cells often reside in local microenvironments, or niches. Although niches can contain multiple types of stem cells, the coordinate regulation of stem cell behavior is poorly understood. In the *Drosophila* testis, Janus kinase–signal transducer and activator of transcription (JAK-STAT) signaling is directly required for maintenance of the resident germline and somatic stem cells. We found that the JAK-STAT signaling target and inhibitor Suppressor of cytokine signaling 36E (SOCS36E) is required for germline stem cell maintenance. SOCS36E suppresses JAK-STAT signaling specifically in the somatic stem cells, preventing them from displacing neighboring germline stem cells in a manner that depends on the adhesion protein integrin. Thus, in niches housing multiple stem cell types, negative feedback loops can modulate signaling, preventing one stem cell population from outcompeting the other.

Adult stem cells reside in local microenvironments, or niches, in which signals from surrounding stromal cells inhibit differentiation (*1*). Niches are often structurally and molecularly complex, with diverse signaling pathways operating in a given niche (*2*). In niches containing multiple types of stem cells, it is unclear how behavior is coordinated to produce an appropriate ratio of differentiated cell types (*3*). Among the best-characterized niches are those in the *Drosophila* gonads, in which germline and

somatic stem cells cooperate during gametogenesis (*3*, *4*). In the ovary, germline stem cells (GSCs) and somatic stem cells (called escort stem cells) share a niche. However, separate signals appear to regulate escort stem cell and GSC maintenance (*5*). In the testis, germline and somatic stem cells (cyst progenitor cells, or CPCs) reside in a single niche created by a small cluster of stromal cells (the hub) (fig. S1A), and both require Janus kinase-signal transducer and activator of transcription (JAK-STAT) signaling for their maintenance (*6–8*).

Thus, the *Drosophila* testis provides a tractable paradigm for understanding the coordinate regulation of multiple stem cell types within a single niche.

Because JAK-STAT signaling is directly required for GSC and CPC maintenance in the *Drosophila* testis (fig. S2 and table S1) (*6–8*), studying STAT targets should reveal regulatory mechanisms in one or both stem cell lineages. Transcriptional profiling identified putative STAT targets in this niche, including the JAK-STAT inhibitor Suppressor of cytokine signaling 36E (SOCS36E) (*9*). *socs36E* is expressed specifically at high levels in the hub and at lower levels in CPCs (fig. S1B) (*9*), making it an excellent candidate regulator within the testis niche.

SOCS proteins, first identified in vertebrates, are highly conserved antagonists of JAK-STAT signaling that act in a classic negative feedback loop: In response to signal activation, SOCS proteins bind and inhibit JAK kinases or their associated receptors so as to down-regulate the pathway

Department of Cell Biology, Johns Hopkins University School of Medicine, 725 North Wolfe Street, Baltimore, MD 21205, USA.

*Present address: Department of Neuroscience, University of Pennsylvania School of Medicine, 232 Stemmler Hall, Philadelphia, PA 19104, USA.
†Present address: Department of Biochemistry and Molecular Biology, University of Chicago, 929 East 57th Street, Chicago, IL 60637, USA.
‡To whom correspondence should be addressed. E-mail: matunis@jhmi.edu